

163

METEOROLOGICAL OFFICE

Scientific Paper No. 16

An Experiment in Operational Numerical Weather Prediction

by E. KNIGHTING, B.Sc., G. A. CORBY, B.Sc.,
and P. R. ROWNTREE, B.A.

LONDON: HER MAJESTY'S STATIONERY OFFICE
THREE SHILLINGS NET

METEOROLOGICAL OFFICE

Scientific Paper No. 16

An Experiment in Operational Numerical Weather Prediction

by E. KNIGHTING, B.Sc., G. A. CORBY, B.Sc.
and P. R. ROWNTREE, B.A.

LONDON
HER MAJESTY'S STATIONERY OFFICE
1962

Contents

Introduction	1
The model used in the experiments	2
Objective analysis and data extraction	5
Verification of the forecast charts	13
Some examples of the numerical forecasts ..	19
Conclusions	20
Bibliography	21

An Experiment in Operational Numerical Weather Prediction

by E. Knighting, B.Sc., G. A. Corby, B.Sc. and P. R. Rowntree, B.A.

INTRODUCTION

A series of experiments in numerical forecasting of the wind and pressure fields has been carried out since the installation of the Meteorological Office electronic computer, a Ferranti Mercury machine known as METEOR, in January 1959. Reports of these experiments are given by Knighting *et alii*¹*, Knighting and Hinds², Bushby and Whitlam³, Corby⁴, and Knighting⁵, and the results indicated that a satisfactory method of automatic analysis had been achieved and that the three-parameter model atmosphere yielded better results than the other models that had been used as a basis for the numerical integrations.

As a result of these experiments it was decided that an experiment should be mounted with the object of providing numerical forecasts to an operational schedule; in particular, this meant that a prebaratic[†] referring to 0600 GMT on the following day should be available to the forecasting staff by 0930 GMT. It was clear from the previous experiments that the three-parameter model, described below, was the most suitable model available for carrying out the numerical integrations.

The decision to carry out such an experiment posed various problems, mainly in the preparation and analysis of data. The existing techniques of automatic data extraction were designed for use with a two-parameter model and needed considerable modification to meet the needs of a three-parameter model; moreover, the techniques were specifically related to extraction from a high quality bulletin (Knighting *et alii*¹, page 8) which unfortunately was broadcast too late to be of use in an operational experiment. It seemed desirable, since the time schedule allowed, to use such 0600 GMT data as were available in the routine, as described below, and the problem of the extraction and use of such data posed new problems.

The available objective analysis techniques had also been developed for a two-parameter model and needed extending for use with a three-parameter model, while at the same time problems of computer memory space concerning the three-parameter model itself had to be resolved.

It was decided quite early in the preparations for the experiment that the problem of automatic data extraction of the midnight data from heterogeneous meteorological broadcasts was so complicated that its study would require much time and if actively pursued as an element of the experiment would delay commencement of the trials. Most of these data were therefore extracted manually and punched on paper tape, leaving the problems of the later data referring to 0600 GMT for solution.

The experiment as conceived consisted essentially of a six-hour forecast based upon the midnight data, followed by a new analysis based upon this six-hour forecast and such

*The superscript figures refer to the bibliography on page 21.

†A forecast chart.

0600 GMT data as were available, followed by a 24-hour forecast based upon this new analysis. The time schedule, obtained by working backwards from the proposed time of issue of the completed results, required close consideration so as to allow the use of the maximum amount of available 0600 GMT data and had to be adhered to within a few minutes. It was not possible to maintain the time schedule on all occasions due to faults in the computer and various difficulties encountered in dealing with the extraction of data. The forecast was ready by 0930 GMT on about 35 per cent of occasions and by 0945 GMT on another 20 per cent. On more than 30 occasions computer faults caused either delay in computing the forecast or abandonment of the computation; the faults were often quickly located and would not have much affected research projects. It became clear that a more reliable computer than METEOR is necessary if routine computations are to be carried out to a strict time schedule.

The programmes were written and tested before the end of October 1960 and the experiment commenced, after the assembly of the necessary ancillary staff, on 21 November 1960 and ended on 9 June 1961 when preparations started on the dismantling of METEOR for removal to the new headquarters at Bracknell. Numerical forecasts were made on Tuesday to Friday of each week and the total number of verified 1000 mb forecasts was 107.

THE MODEL USED IN THE EXPERIMENTS

Basic assumptions

The three-parameter model used in the experiments was that described by Bushby and Whitlam³. Briefly it consists of two layers of shearing fluid bounded respectively by the pressure surfaces p_0 (=1000 mb), p_m (=600 mb) and p_1 (=200 mb). Within each layer the thermal wind is assumed to be constant in direction and to vary linearly with pressure. The winds are obtained from the geostrophic relationship. The vertical motion is assumed to vary parabolically with pressure in each layer, with $\bar{\omega}$ ($=dp/dt$) and $\partial\bar{\omega}/\partial p$ continuous at the interface; at the boundaries p_0 and p_1 , $\bar{\omega}$ is assumed to vanish. The non-adiabatic heating of cold air over warm sea was taken to be confined to the lower layer and both the twisting term and the vertical advection of vorticity were neglected as in the previous experiments described by Knighting *et alii*¹.

Equations

The relevant equations, referred to a stereographic projection from the South Pole onto a tangent plane at the North Pole, are given by Bushby and Whitlam³; they are

$$\begin{aligned} \nabla^2 \left\{ \frac{\partial h_m}{\partial t} + \frac{1}{4} \left(\frac{\partial h_1'}{\partial t} - \frac{\partial h_0'}{\partial t} \right) \right\} + J [h_m, \beta^2 g f^{-1} \nabla^2 \{ h_m + \frac{1}{4}(h_1' - h_0') \} + f] \\ + \frac{1}{4} J(h_1' - h_0', \beta^2 g f^{-1} \nabla^2 h_m + f) + \frac{1}{8} \{ J(h_0', \beta^2 g f^{-1} \nabla^2 h_0') \\ + J(h_1', \beta^2 g f^{-1} \nabla^2 h_1') \} = 0 \end{aligned} \quad (1)$$

$$\begin{aligned} \nabla^2 \frac{\partial h_0'}{\partial t} + J(h_m, \beta^2 g f^{-1} \nabla^2 h_0') + J \{ h_0', \beta^2 g f^{-1} \nabla^2 (h_m - h_0') + f \} \\ = - \frac{2(a+b)}{p_0 - p_1} \left\{ 2 \left(\nabla^2 h_m + \frac{f^2}{\beta^2 g} \right) - \nabla^2 h_0' \right\} \end{aligned} \quad (2)$$

$$\begin{aligned} \nabla^2 \frac{\partial h_1'}{\partial t} + J(h_m, \beta^2 g f^{-1} \nabla^2 h_1') + J\{h_1', \beta^2 g f^{-1} \nabla^2 (h_m + h_1') + f\} \\ = -\frac{2(a-b)}{p_0 - p_1} \left\{ 2 \left(\nabla^2 h_m + \frac{f^2}{\beta^2 g} \right) + \nabla^2 h_1' \right\} \end{aligned} \quad (3)$$

$$\frac{\partial h_0'}{\partial t} = -\beta^2 g f^{-1} J(h_m, h_0') + Q_0 + Aa + Bb \quad (4)$$

$$\frac{\partial h_1'}{\partial t} = -\beta^2 g f^{-1} J(h_m, h_1') + Ca + Db \quad (5)$$

$$H_1 = H_0 + \left(\frac{\partial H}{\partial t} \right)_0 \delta t \quad (6)$$

$$H_{r+1} = H_{r-1} + 2 \left(\frac{\partial H}{\partial t} \right)_r \delta t \quad (7)$$

where h_m = contour height at 600 mb

h_0' = 1000–600 mb thickness

h_1' = 600–200 mb thickness

a, b = characterise $\bar{\omega}$ in the lower and upper layers respectively

A, B, C, D = absolute constants of the model

and the remainder of the symbols are as defined by Knighting *et alii*¹, with suffixes 0 or 1 if required, referring respectively to the lower and upper layers. In these equations the unknowns are $\partial h_m / \partial t$, $\partial h_0' / \partial t$, $\partial h_1' / \partial t$, a and b .

The basic data required to start the integrations are the values of h_m , h_0' and h_1' . The actual data available after the objective analysis are the 500 mb contour height and the 1000–500 mb and 500–200 mb thicknesses. The required data are then defined by

$$\begin{aligned} h_m &= h_{500} - \frac{1}{5} h'_{500} \\ h_0' &= \frac{4}{5} h'_{500} \\ h_1' &= h_{200} - h_m \end{aligned} \quad (8)$$

These definitions do not, of course, provide good estimates of h_m , h_0' , h_1' but they do provide good estimates of the gradients of these quantities, which enter into the prognostic equations. At the end of the forecast h_{1000} , h_{500} and h_{200} were obtained through the relations (8). The empirical allowance for heating of the lower layer of air over the sea was the same as that given by Bushby and Hinds⁶.

The equations (1) to (5) are a simple generalization of equations (1) to (3) in Knighting *et alii*¹. Equations (1) of the two papers correspond whilst equations (2) and (3) above express

the changes of thermal vorticity in the two layers and correspond to the simple equation (2) in the paper cited, and equations (4) and (5) express the changes of thickness in the two layers and correspond to equation (3).

Method of solution

The prognostic equations were solved over a rectangular grid of 24×20 points (Figure 2), the grid length being approximately 200 statute miles at the North Pole. The differential equations were replaced by the simple finite difference schemes

$$\frac{\partial z_0}{\partial x} = \frac{z_1 - z_3}{2d}, \quad \frac{\partial z_0}{\partial y} = \frac{z_2 - z_4}{2d}$$

$$\nabla^2 z = \frac{\sum_{i=1}^4 z_i - 4z_0}{d^2}$$

$$J(X, Y)_0 = \frac{(X_1 - X_3)(Y_2 - Y_4) - (Y_1 - Y_3)(X_2 - X_4)}{4d^2} \quad (9)$$

where d is the grid length and the suffixes refer to the points in Figure 1.

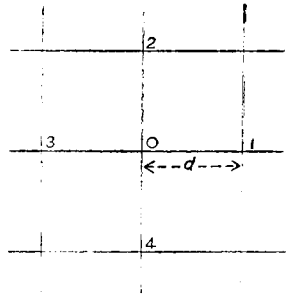


FIGURE 1. Suffix notation relative to origin, O

Equations (4) and (5) are linear in a and b and substituting their values in equations (2) and (3) yields the simultaneous equations

$$\nabla^2 \frac{\partial h_0'}{\partial t} + E \frac{\partial h_0'}{\partial t} + F \frac{\partial h_1'}{\partial t} + G = 0 \quad (10)$$

$$\nabla^2 \frac{\partial h_1'}{\partial t} + L \frac{\partial h_0'}{\partial t} + M \frac{\partial h_1'}{\partial t} + N = 0 \quad (11)$$

where E, F, G, L, M, N are functions of the derivatives of h_m, h_0', h_1' and known parameters. The finite difference forms of these equations were solved simultaneously for $\partial h_0'/\partial t$ and $\partial h_1'/\partial t$ by the Liebmann iterative process, assuming that $\partial h_0'/\partial t, \partial h_1'/\partial t = 0$ on the boundary. The finite difference form of equation (1) was then solved for $\partial h_m/\partial t + \frac{1}{2}(\partial h_1'/\partial t - \partial h_0'/\partial t)$ assuming additionally that $\partial h_m/\partial t = 0$ on the boundary. With an initial guess of $\partial h_0'/\partial t, \partial h_1'/\partial t, \partial h_m/\partial t = 0$ at the interior grid points about 18 and 30 iterations were usually required

in order that the solutions satisfied the test that the sum of the residuals was less than one metre per hour; at subsequent time-steps the last computed values of the tendencies were sufficiently good approximations to the solution as to require only 3–6 iterations before the criterion was satisfied. When required, the values of a and b may be obtained from equations (4) and (5).

The time step was taken to be $\frac{3}{4}$ hour and the computation of the new fields of contour height and thickness from those at the previous time step took about $1\frac{1}{4}$ minutes.

OBJECTIVE ANALYSIS AND DATA EXTRACTION

General scheme

The end product of the experiment, namely a numerical forecast for 0600 GMT on the day following computation, proceeded from objective analyses of the contour charts for 0000 GMT. As already indicated, however, the 30-hour forecast was interrupted after it had proceeded for six hours (real, not computing time) in order that such 0600 GMT data, upper air and surface, as had been received by the appropriate time could be exploited to correct the forecast so far obtained. Essentially this required additional objective analysis computations for the 0600 GMT data. A considerable quantity of data, both upper air and surface, for both 0000 and 0600 GMT was therefore required to be fed into the computer. Practical considerations necessitated a mixture of manual and automatic extraction of the data and a large part of the available effort was concerned with the data handling side of the experiment.

0000 GMT analyses

Upper air data were extracted manually from the teleprinter messages. The data comprised contour heights for 1000, 500 and 200 mb and wind speeds and directions for 850, 500 and 200 mb from as many stations as possible from a target list of 208 stations excluding the ocean weather ships. Extraction and punching of the data on tape proceeded concurrently so that by some time approaching 0700 GMT the data tape was ready for reading into the computer. The choice of a manual extraction system for these data was adopted because the only scheme of automatic data extraction already developed was designed to operate on ABTOP messages and the data were not received in that form sufficiently early for the target time for the completion of the computation to be attainable. It was decided therefore not to delay the experiment whilst a more comprehensive scheme of automatic data extraction, able to cope with other broadcasts, was developed.

The upper air data having been input to the computer, the basic method used for the 0000 GMT upper air analyses followed that proposed by Bushby and Huckle⁷ and used for the previous experiment described by Knighting *et alii*¹. This involved each grid point being dealt with individually, a second degree polynomial being fitted to the data in the vicinity of each point by least squares. The computation was, however, extended to improve on the use of the geostrophic approximation in the fitting of wind observations and to include the other modifications proposed by Corby⁴ as a means of achieving better analyses in the region of deep depressions. These additions to the computation necessitated the analysis being computed twice and, as in the previous experiment, the first analysis was used as a basis for the application of certain tests to the data, any erroneous observations so found being ignored during the second analysis. For the 1000–500 mb thickness field, and the 500 mb and 200 mb levels the whole process occupied the computer for about 25 minutes.

The implied 1000 mb analysis so obtained was, as in the previous experiment¹, adequate over the land areas where the density of upper air stations is good but was too smooth and lacking in detail over the Atlantic Ocean. To overcome this shortcoming the next stage in the process comprised an analysis of all the available surface observations of wind and pressure from ships on the Atlantic; typically there were upwards of 100 such observations. In the case of these data automatic extraction by the computer was possible from punched tapes arising in the Meteorological Office communications section. The analysis process followed the same lines as already indicated, including the additional measures devised to achieve better analyses in the vicinity of deep depressions. On completion of this 1000 mb analysis, the 1000–500 mb thickness and 500 mb analyses as previously found were adjusted, grid point by grid point, to render them consistent with the revised 1000 mb analysis. Automatic extraction of the surface observations from ships and the additional analysis computations occupied the computer for a further 25 minutes approximately. This was followed by a six-hour numerical forecast for the three levels, requiring about 12 minutes computation, and after this stage the forecast was halted to allow use to be made of 0600 GMT data. (See page 2 for a description of the forecasting model and procedure.)

0600 GMT analyses

Although there is full coverage of surface observations for 0600 GMT the upper air data for this time comprises upper winds from a few stations only, mainly the British stations, Gibraltar and the ocean weather ships. It was thought that it should be worth while to make use of these upper data, although limited, but the analysis process normally adopted, involving the individual fitting of a quadric surface to the data in the vicinity of each grid point, would clearly have been wasteful of computing time having regard to the small number of data. What was required was a more simple process to correct the gradients of contour height in the six-hour forecast from 0000 GMT, so as to accommodate these 0600 GMT upper wind observations. It was decided for this purpose to adopt a scheme on the lines of that used at the Joint Numerical Weather Prediction Unit and described by Cressman⁸. In this process the analysed value for a grid point is derived as a linear combination of various estimates made from the data and thus it is possible to arrange the computation observation by observation rather than grid point by grid point. This greatly speeds up the calculation when the data are scanty.

In brief the process was operated as follows. Contour height values were interpolated at the positions of the wind observations from the field to be modified, namely the six-hour forecast. From each wind observation, estimates of the contour height at neighbouring grid points were then obtained by simple extrapolation using the geostrophic wind equation. In addition to the original value a number of such estimates were thus available at each grid point, and a modified value was formed as a linear combination of these. This took the form:

$$\frac{(n - \sum W)h_G + \sum Wh}{n}$$

where h_G is the original value at the grid point, h a value estimated using a wind observation, W a distance weighting function (maximum value 1) and n the number of observations. Following Cressman⁸ the form used for W was

$$W = \frac{N^2 - d^2}{N^2 + d^2}$$

where N is the range over which the observation was allowed to have effect and d the distance between observation and grid point. For $d > N$, W was taken to be zero. This process was iterated, a fresh contour height value for association with each wind observation being interpolated before each scan and the value of N^2 being successively reduced. Four scans were carried out, the values of N^2 used being successively 25, 16, 9 and 5. The aim of this was to correct the grossest errors on the first scan and progressively to fit the winds more closely in their immediate vicinity during the later scans. In Cressman's description of the process slightly different values of N^2 are referred to and smoothing operators were applied at various stages in the process. However, making use of a small number of upper wind observations only is rather different from the analysis of a full coverage of both contour heights and winds and the values of N^2 were adopted after some preliminary experiments in the fitting of a sparse network of winds alone. A procedure for the testing of the data against the current field before each scan was incorporated. This was simply a comparison between the observed wind and a geostrophic wind interpolated from the current field, the observation being rejected if the discrepancy exceeded specified limits. The criteria used were 90 knots before the first scan, 70 knots before the second, 60 knots before the third and 50 knots before the fourth and final scan. These values may seem rather high but the method may only be applied for the detection of rather gross errors. The small amount of data required for this analysis of 0600 GMT upper wind observations was extracted and punched on paper tape manually. The computation occupied about five minutes for the three fields 1000–500 mb thickness, 500 mb and 200 mb.

The next stage in the procedure was an analysis of the 0600 GMT surface observations using as a first guess the current 1000 mb field as implied by the 500 mb and 1000–500 mb thickness fields. The technique used here was once again the full quadric fitting process applied to each grid point in turn. The data comprised surface pressures from all available land stations from a target list of 192 stations, together with observations of surface pressure and wind from ships. In all cases surface temperatures were also used for the conversion of surface pressures to 1000 mb heights. Data for the land stations were extracted and punched on tape by hand whilst the ship data were extracted automatically. In other respects the procedure followed the same lines as for the 0000 GMT 1000 mb analysis, including the adjustments to the upper fields to render them consistent with the surface field. The 0600 GMT 1000 mb analysis, including input of data and output of results occupied the computer for about 30 minutes.

Timetable for the experiment

In the absence of delays due to faulty data tapes, etc. the timetable typically ran as follows:

Time GMT	Commencement of:
0700	0000 GMT analysis of three upper levels
0725	Automatic extraction of 0000 GMT surface observations from ships
0730	0000 GMT 1000 mb analysis
0750	Six-hour numerical forecast
0802	Adjustments to accommodate 0600 GMT upper wind observations
0807	Automatic extraction of 0600 GMT surface observations from ships
0812	0600 GMT 1000 mb analysis
0837	24-hour numerical forecast, making 30-hours from 0000 GMT
0925	(End of computation).

These times relate to the operation of the computer. The manual extraction of 0000 GMT upper air data for three levels from about 200 stations and the punching of these data on tape

occupied two assistant staff from about 0100 GMT, when receipt of the data commenced, until almost 0700 GMT, the deadline for input of the data to the computer. Similar work for the 0600 GMT surface observations from land stations was carried out between 0700 and 0800 GMT. In these two cases the bulk of the data was in fact normally available in time to meet the deadline. The punched tapes bearing the 0000 GMT surface observations from ships were also available in ample time for the computation. However, in the case of the 0600 GMT surface observations from ships these were still being received in appreciable numbers at the time, soon after 0800 GMT, when it was necessary to be ready for the computation of the 0600 GMT surface analysis. Waiting for further data would have made it impossible to complete the forecast on time. The speed of the computer is relevant here—a faster machine would permit the forecast computation to be commenced later and therefore would allow more data to be used.

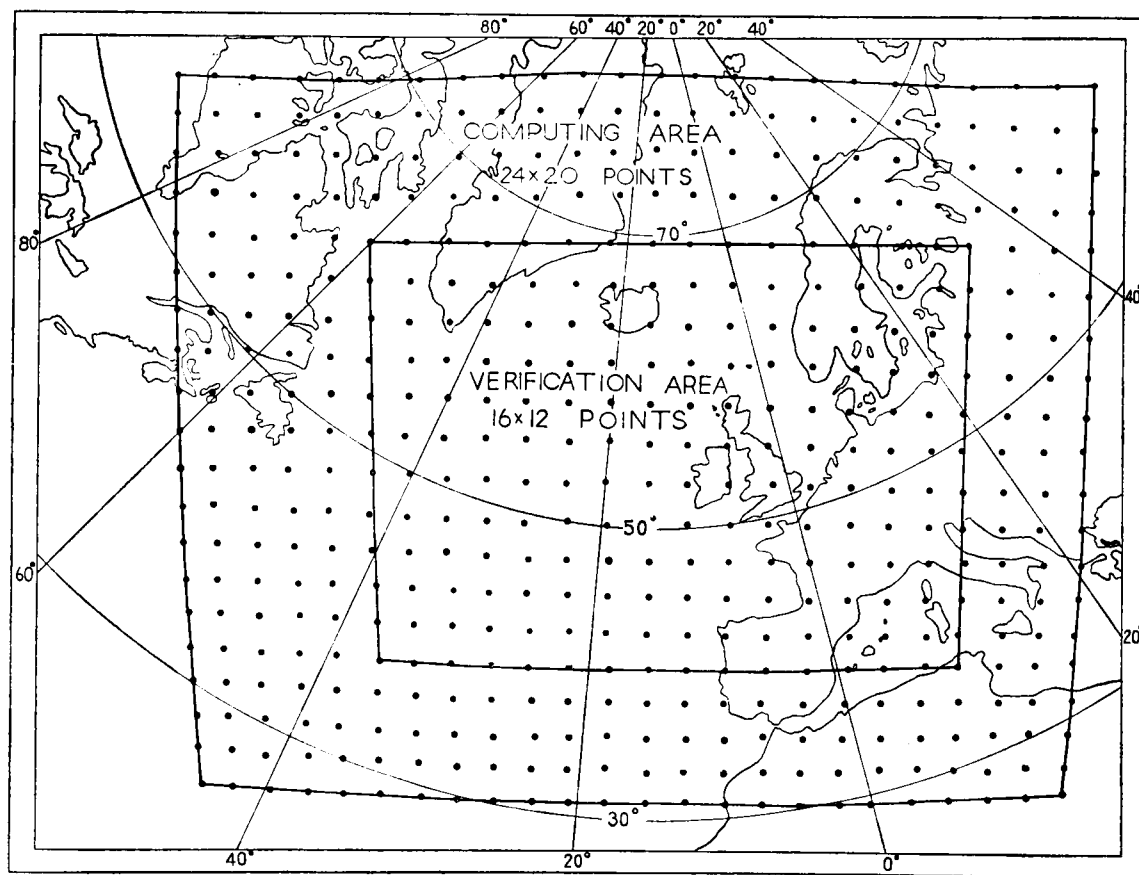


FIGURE 2. Computing grid for numerical forecasting experiment.

The grid points form a square network on a stereographic projection from the South Pole on to a plane perpendicular to the earth's axis.

Grid length = $88.1412 (1 + \sin \theta)$ nautical miles, where θ is the latitude
 = 176 n.miles (325 km) at the North Pole
 = 164 n.miles (303 km) at 60°N
 = 132 n.miles (244 km) at 30°N

Quality of the analyses

The experiment included upper air analyses for three levels and surface analyses for both 0000 GMT and 0600 GMT so that there were considerable opportunities for verification of the analyses. However, if full-scale statistical comparison with subjectively analysed charts is undertaken it is necessary to read off large numbers of contour height values at the grid points from the manually drawn charts and punch these on tape. The effort entailed was too great in an experiment running on an almost daily basis and the analysis verification programme was therefore limited to the 0600 GMT surface analyses. Grid point values were read off from the subjectively drawn 0600 GMT surface charts, punched on tape and various statistical comparisons were made with the corresponding computed analyses. The area for these comparisons was the inner 16×12 grid as used for the verification of the forecasts (Figure 2). Values read from the subjective charts were in millibars and these were converted to 1000 mb heights within the computer, using values of monthly mean thickness at the grid points as a guide to the surface temperature.

The root mean square (r.m.s.) discrepancy of 1000 mb contour height, evaluated over the 16×12 grid and over 107 cases for which comparison was possible, amounted to 24 metres. This is of the same order as the human variation in chart analysis and must to some extent comprise the inevitable uncertainty of analysis over an area of which a large part is ocean. The verification charts were not specially prepared but were the normal operational charts drawn as part of the daily routine of the forecast division. Furthermore values for verification were only read off to the nearest millibar (approximately eight metres in terms of 1000 mb contour height). Thus the figure of 24 metres includes several unavoidable uncertainties as well as the actual error of the computed analyses.

Figure 3, which gives the frequency distribution of r.m.s. contour height discrepancy for the 107 analyses, shows a fairly wide spread from 12 metres to 42 metres. The former figure represents exceedingly close agreement between the computed and manual analyses and tended to be confined to summer situations devoid of intense systems and also of undetected data errors. The very large discrepancies occurred in situations with very deep systems over the ocean, usually accompanied by some difficulties with the data. As an example very large discrepancies arose in the 0600 GMT analysis for 1 February 1961, resulting in an overall r.m.s. discrepancy from the manual analysis of 42 metres. This was almost entirely due to differences in the analysis of a very deep depression in mid-Atlantic and as it illustrates the kind of difficulty which occurs in objective analysis a few details of this case are given.

The relevant portion of the subjective analysis is illustrated in Figure 4(a) together with the pressure and wind observations from ships within about 700 miles of the depression centre, as available to the forecaster. It will be seen that there were only eight observations in the area and of these the forecaster ignored the pressure reported at 49.2°N 49.4°W and treated the pressure at 44.0°N 41.0°W as 10 mb too high. Furthermore, it is clear that in analysing the position of the main centre and the presence of the secondary centre at the tip of the warm sector the forecaster must have been strongly influenced by history or preconceived ideas, as the data alone do not lead inevitably to the analysis adopted. The corresponding objective analysis of the same portion of the chart, together with the data available for the calculation, is given at Figure 4(b). Of the eight observations available to the forecaster, three were not received in time for the objective analysis, and one of the remainder, at 52.1°N 32.1°W , was received corrupt and was not successfully decoded by the computer programme. Furthermore the 10 mb pressure error at 44°N 41°W was not detected within

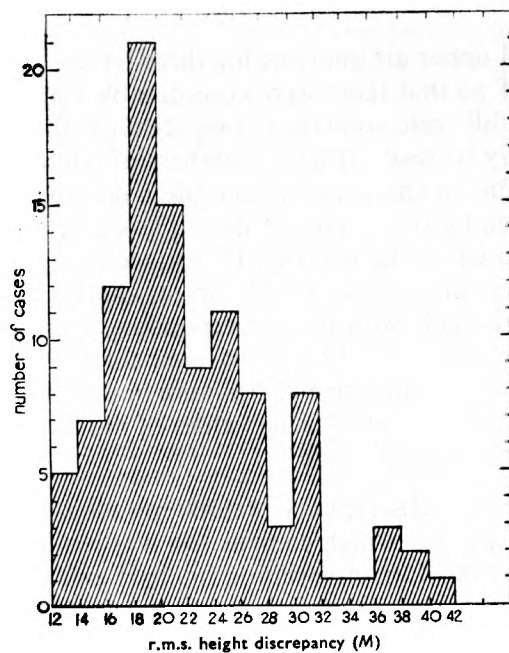


FIGURE 3. Frequency distribution of r.m.s. discrepancies between objective and subjective 1000 mb analyses at 0600 GMT evaluated over the 16×12 grid for 107 analyses

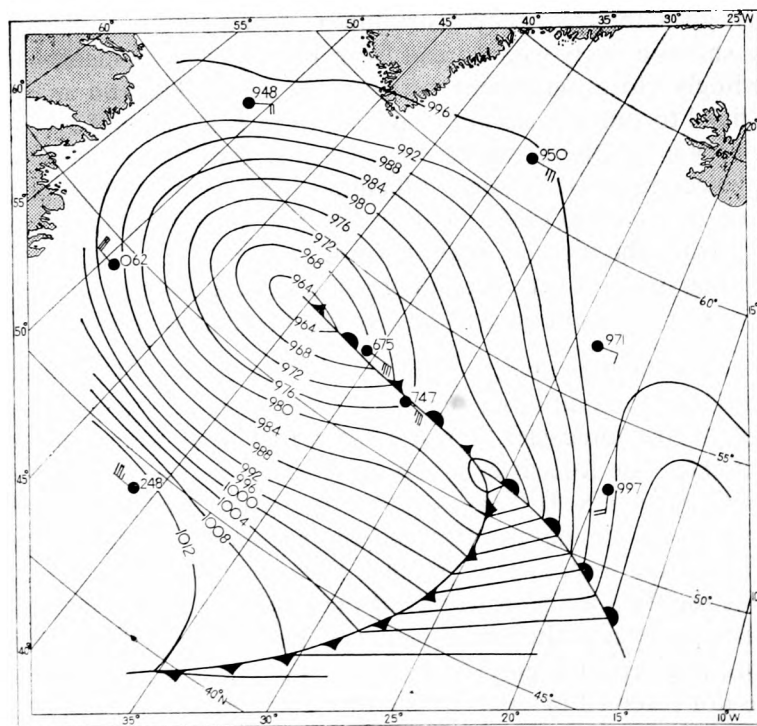


FIGURE 4(a). Portion of subjective (C.F.O.) surface analysis for 0600 GMT, 1 February 1961 with available ships' observations of pressure and wind

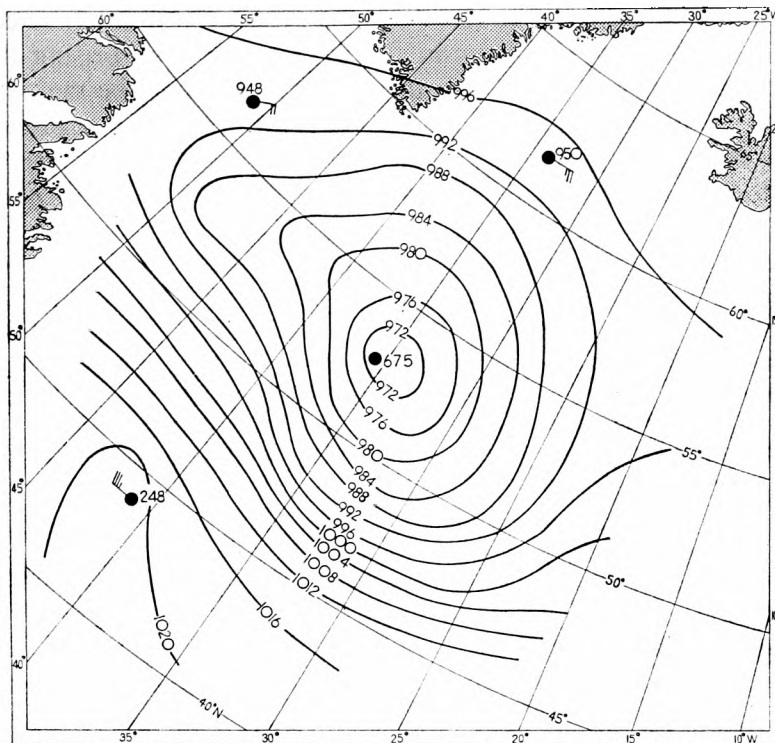


FIGURE 4(b). Portion of objective surface analysis for 0600 GMT, 1 February 1961 with ships' observations available to computer

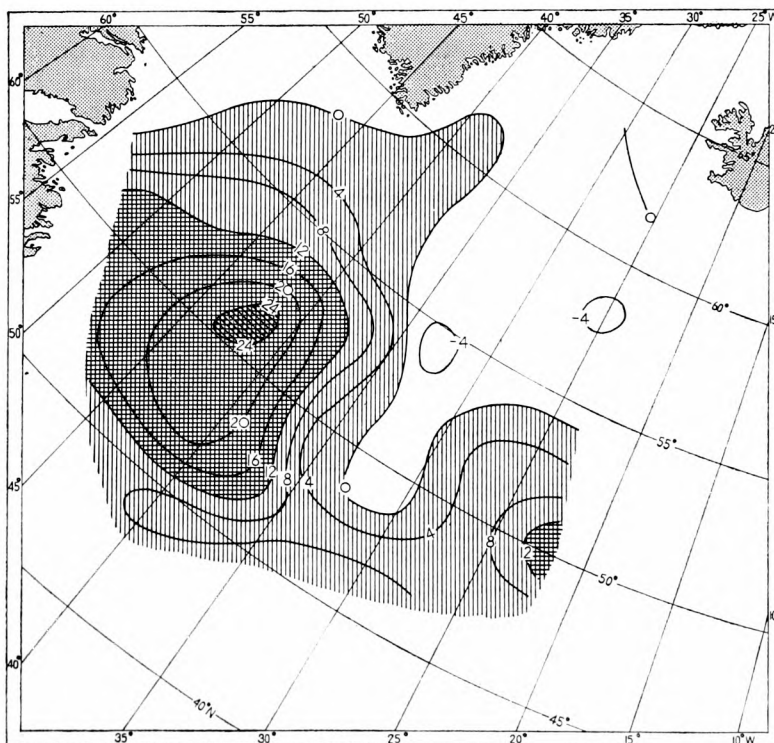


FIGURE 4(c). Isoleths of discrepancy (mb) between objective and subjective surface analyses for 0600 GMT, 1 February 1961

the computer and the wind reported at $52.8^{\circ}\text{N } 35.5^{\circ}\text{W}$ was unfortunately rejected as probably spurious. In the face of these variations in the data it is not surprising that the analyses differed. The main differences were that in the objective analysis the main centre was a few millibars less deep and about one grid length east-south-east of the subjectively analysed position, whilst a ridge was erroneously introduced into the south-west quadrant of the depression, chiefly owing to the incorrect pressure report from $44^{\circ}\text{N } 41^{\circ}\text{W}$. The field of discrepancy between the two analyses is illustrated in Figure 4(c) which shows that large differences, reaching a peak value of 24 mb, occurred near the centre and in the south-west quadrant. Such differences can readily arise when there are steep gradients and errors in the position of systems are made. The overall r.m.s. discrepancy of 42 metres (approximately 5 mb) in this case was the largest occurring during the whole experiment.

Most of the cases in which large analysis discrepancies of this sort occurred in the 0600 GMT surface analyses were in some way or other associated with difficulties of the data—undetected errors of substance or of ship's positions or merely unusual sparseness leading to inevitable differences of interpretation.

In addition to the height errors, the r.m.s. discrepancies of geostrophic wind between the objective and subjective analyses were evaluated over the 16×12 grid in each case, giving values which ranged from 7 knots to 20 knots with an overall r.m.s. value for the 107 cases of 12.7 knots. According to Murray⁹, the errors inherent in charting techniques amount to 9 knots (r.m.s. value) over the British Isles at 500 mb and if other factors are allowed for, e.g. ageostrophic components, etc., the r.m.s. difference between observed winds and geostrophic winds measured from manually drawn charts rises to 14 knots. Although not directly relevant, these figures suggest that the overall r.m.s. discrepancy between the objective and subjective analyses of 12.7 knots implies a satisfactory standard of analysis in the mean. As in the case of the contour height discrepancies, however, large errors occurred on some occasions over limited areas, due very largely to undetected data errors. Indeed, to achieve uniformly high quality objective analyses the need now is much more for superior procedures for the detection of data errors than for improved techniques of analysis.

So far we have been considering the 0600 GMT surface analyses but the quality of these was not only determined by the 0600 GMT surface observations and the treatment thereof. The analyses were inevitably coloured by the preceding computations from the 0000 GMT analysis onwards, especially over areas with little or no 0600 GMT surface data. Thus errors in the six-hour forecast from 0000 GMT as well as errors in the previous analyses often played some part in causing discrepancies in the 0600 GMT surface analyses, especially over the Atlantic. In particular the process used to exploit the small number of upper wind observations at 0600 GMT, although beneficial in the mean, was found during the course of the experiment to be rather unsatisfactory and sometimes gave rise to large errors which indirectly contaminated the 0600 GMT surface analysis. The process in question involved linear extrapolation using estimated contour gradients obtained from the observed winds. Such linear extrapolation can readily give rise to large errors especially if the extrapolation proceeds from an observation on one side of a low or sharp trough to a grid point on the other. If the range of effect of an observation is limited too much in order to reduce such errors, spurious short-wavelength features tend to be introduced in the vicinity of the wind observations, and rather subtle restraints are required if any process involving linear extrapolation is to be acceptable. These faults were not fully appreciated during the running of the experiment and the process would need overhauling before further use in the future.

VERIFICATION OF THE FORECAST CHARTS

Following the results established by Wallington¹⁰ an extended verification programme was written to compute statistical measures of the agreement between the forecast chart and its verifying chart over the inner verification area shown in Figure 2. The verifying chart was taken to be the chart constructed by the Central Forecasting Office (C.F.O.) and this entailed the reading and punching on paper tape of the grid point values of the verifying chart; this extraction process was also carried out for the C.F.O. prebaratic charts verifiable at the same time. Since the prebaratic referred to 0600 GMT there were no verifying upper air charts, so that the main statistics refer only to the 1000 mb chart. Additionally the upper air charts were verified against the objective analysis referring to the verifying time, i.e. 0000 GMT. It was not possible to extract all the corresponding data from the C.F.O. upper air forecasts, so that the statistics referring to all the upper air forecasts can only be compared with a forecast of persistence. However, in 30 cases the C.F.O. forecast data have been extracted and the corresponding statistics are presented.

The statistics presented here are:

- (i) Correlation coefficient between the forecast and actual contour height changes.
- (ii) Root mean square error in the forecast contour heights.
- (iii) Root mean square vector error in the forecast geostrophic winds measured over single grid lengths.
- (iv) Stretch vector correlation between the forecast and verifying geostrophic winds measured over single grid lengths.
- (v) Wind equivalent to the difference between the forecast and actual mean square geostrophic wind, i.e.

$$V_s^2 = \overline{V_f \cdot V_f} - \overline{V_a \cdot V_a} \quad (12)$$

where V_s is the statistic, V_f the forecast geostrophic wind, V_a the verifying geostrophic wind and the bar indicates a mean.

Each of the terms in equation (12) is akin to a kinetic energy and V_s^2 indicates the excess (or deficit) of the forecast kinetic energy over the verifying value. The sign accorded to V_s was that of the right-hand side, so that a positive value of V_s indicates that the forecast overestimated the kinetic energy and vice versa.

The forecasts were made on Tuesday, Wednesday, Thursday and Friday. It was then possible to verify the 1000 mb forecast made on each of these four days against the appropriate verifying charts for the following days. No objective analysis was made on Saturday so that the upper air forecasts were verified only for the forecasts made on Tuesday, Wednesday and Thursday. For the purpose of verification the experiment was divided into two parts, 22 November 1960–3 March 1961 and 7 March 1961–8 June 1961, representative of winter and spring-summer.

The following tables give the mean statistics for the experiment. Table I shows the mean statistics for the 24-hour 1000 mb forecasts compared with persistence and the 30-hour 1000 mb forecasts compared both with persistence and the C.F.O. forecasts. There is an indication that the forecast errors given in rows 2, 3 and 5 increase linearly with time, although this is not necessarily true of individual forecasts. The errors in persistence do not indicate

TABLE I. Mean statistics for forecasts at 1000 mb

24 hr forecast for 0000 GMT compared with objective analysis							30 hr forecast for 0600 GMT compared with C.F.O. analysis								
Numerical forecast			Persistence				Numerical forecast			C.F.O. forecast (24 hr)			Persistence (24 hr)		
	(a)	(b)	(c)	(a)	(b)	(c)	(d)	(e)	(f)	(d)	(e)	(f)	(d)	(e)	(f)
1.	0.80	0.71	0.74	—	—	—	0.56	0.54	0.55	0.67	0.68	0.67	—	—	—
2.	63	47	56	81	57	71	88	61	76	59	44	53	75	57	67
3.	26	20	23	31	23	27	33	25	29	23	17	21	29	22	26
4.	0.70	0.71	0.68	0.40	0.52	0.45	0.53	0.58	0.55	0.61	0.69	0.65	0.42	0.51	0.46
5.	20	15	18	4	0	2	25	20	23	—5	—5	—5	1	1	1

1. Correlation coefficient between forecast and actual contour height changes
2. R.m.s. error in forecast contour heights (m)
3. R.m.s. vector error in forecast geostrophic wind (kt)
4. Stretch vector correlation between forecast and verifying geostrophic wind
5. Equivalent wind difference between forecast and verifying geostrophic wind (kt)—see p. 13
 - (a) for 42 winter cases
 - (b) for 37 spring cases
 - (c) for total 79 cases
 - (d) for 56 winter cases
 - (e) for 51 spring cases
 - (f) for total 107 cases

a similar linear increase, both being taken over 24 hr. However, the 24-hour numerical forecast is generally superior, as measured by these statistics, to a forecast of persistence but the 30-hour numerical forecast appears to be inferior. It should be recalled that these statistics only measure in part the value of a forecast when considered synoptically. On the other hand the C.F.O. forecasts, which are based upon much more 0600 GMT data than are the numerical forecasts and should be regarded more as 24-hour than 30-hour forecasts, are superior in all statistical measures to the 30-hour numerical forecasts. The statistics for the C.F.O. forecasts are comparable with those of the 24-hour numerical forecast except for the figures relating to kinetic energy, which is small and negative in the C.F.O. forecasts. In view of the previously reported statistics relating to 24-hour forecasts given by Knighting *et alii*¹ which showed great similarity between the statistics relating to 24-hour forecasts made by C.F.O. and by computation, it is pertinent to ask whether the introduction of new data at 0600 GMT materially affects the 30-hour forecast. A few 30-hour forecasts have been computed excluding the revision of the analysis at 0600 GMT and the results are given in Table II;

TABLE II. Mean statistics for 30 hr forecasts at 1000 mb including and excluding 0600 GMT revision of analysis (6 cases)

	(a)	(b)	(c)
Correlation between height changes	0.63	0.49	0.59
R.m.s. height error (m)	86	104	87
R.m.s. vector wind error (kt)	35	38	35

(a) Including 0600 GMT revision of analysis

(b) Excluding 0600 GMT revision of analysis

(c) Including 0600 GMT revision of analysis at 1000 mb but excluding new upper wind data

the occasions occurred in the winter period and seem to indicate that the 0600 GMT re-analysis is worth carrying out even though the gain is small. Similar statistics are included for computations based upon an 0600 GMT analysis which had been revised in the light of the surface data but had omitted the few upper air wind observations available at 0600 GMT; these statistics suggest that the value of including the upper winds is small.

The data necessary for the construction of the statistics were extracted from the C.F.O. forecasts for 0000 GMT for 30 occasions, 15 being selected at random from each half of the experiment; the relevant statistical comparison is given in Table III. Apart from the statistic

TABLE III. *Mean statistics for 24 hr forecasts for 0000 GMT (30 cases)*

	Numerical forecast	C.F.O. forecast	Persistence
1000 mb contours			
1.	0.72	0.73	—
2.	54	48	69
3.	23	19	26
4.	0.68	0.67	0.46
5.	18	—9	1
1000–500 mb thicknesses			
1.	0.79	0.71	—
2.	51	56	67
3.	26	22	25
4.	0.67	0.62	0.41
5.	24	9	0
500 mb contours			
1.	0.77	0.72	—
2.	57	63	83
3.	24	23	30
4.	0.81	0.76	0.60
5.	22	3	2
500–200 mb thicknesses			
1.	0.61	0.53	—
2.	56	52	58
3.	30	20	22
4.	0.37	0.30	0.26
5.	24	—6	0
200 mb contours			
1.	0.77	0.69	—
2.	72	81	103
3.	30	27	33
4.	0.79	0.76	0.61
5.	29	7	2

1. Correlation coefficient between forecast and actual contour height changes
2. R.m.s. error in forecast contour heights (m)
3. R.m.s. vector error in forecast geostrophic wind (kt)
4. Stretch vector correlation between forecast and verifying geostrophic wind
5. Equivalent wind difference between forecast and verifying geostrophic wind (kt)—see p. 13.

relating to kinetic energy, the tabular values show that the numerical forecasts in the upper air are of about the same standard as the conventional forecasts, the statistics numbered 1, 2 and 4 being superior and the r.m.s. wind error being inferior. When these figures are compared with those given by Knighting *et alii*¹ there is an inference that the introduction of 0600 GMT data is beneficial to the forecasting system, although any particular part of the data may have little effect.

Table IV gives the mean statistics for 24-hour numerical forecasts for various levels in the upper air contrasted with those referring to a persistence forecast; it is clear that in most

TABLE IV. *Mean statistics for upper air forecasts*

24 hr forecasts for 0000 GMT compared with objective analysis						
Numerical forecast			Persistence			
	(a)	(b)	(c)	(a)	(b)	(c)
1000-500 mb thicknesses						
1.	0.79	0.78	0.79			
2.	58	47	53	82	57	72
3.	29	23	27	30	22	27
4.	0.62	0.69	0.66	0.31	0.46	0.38
5.	27	22	24	2	1	2
500 mb contours						
1.	0.79	0.76	0.77			
2.	67	51	60	94	71	84
3.	26	21	24	33	25	30
4.	0.80	0.83	0.82	0.55	0.67	0.61
5.	26	21	24	4	5	4
500-200 mb thicknesses						
1.	0.66	0.61	0.64			
2.	66	49	59	73	46	61
3.	35	26	31	26	19	23
4.	0.38	0.38	0.38	0.21	0.33	0.26
5.	27	20	24	0	0	0
200 mb contours						
1.	0.78	0.72	0.75			
2.	85	64	76	121	82	104
3.	35	26	31	37	27	33
4.	0.78	0.80	0.79	0.57	0.69	0.63
5.	36	27	32	3	5	4

1. Correlation coefficient between forecast and actual contour height changes
2. R.m.s. error in forecast contour heights (m)
3. R.m.s. vector error in forecast geostrophic wind (kt)
4. Stretch vector correlation between forecast and verifying geostrophic wind
5. Equivalent wind difference between forecast and verifying geostrophic wind (kt)—see p. 13
 - (a) for 42 winter cases
 - (b) for 37 spring cases
 - (c) for total 79 cases

respects the numerical forecasts are superior, with the exception of the statistics referring to kinetic energy. A notable exception is the r.m.s. wind error for the layer 500–200 mb and it should be noted that the statistics referring to this layer are poorer than those for the other levels and layers, as had been found in a previous experiment (Knighting⁵). The results are similar to those given by Knighting⁵ and suggest that the statistics for the C.F.O. forecasts would not be materially different from those for the numerical forecasts, excepting for the figures relating to kinetic energy.

It is clear from the statistics that the numerical forecasts generally tend to overestimate the kinetic energy within the area of verification and that the overestimation increases with time. On the other hand at 1000 mb the C.F.O. forecasts tend to underestimate the kinetic energy, but to a much less extent than the overestimation given by the numerical forecasts. The corresponding figures for persistence show that in the mean over a large number of cases the kinetic energy is almost unchanged; there are large changes in individual cases. The increase in kinetic energy is not necessarily related with the r.m.s. vector wind error which may arise solely from errors in direction, and although it may not be possible to reduce the r.m.s. vector wind error below the r.m.s. wind difference between two charts analysed by different people, which is of the order of 10 knots, it should be possible to forecast more accurately the mean kinetic energy. In fact the C.F.O. forecasts illustrate this point, since the r.m.s. wind error is 21 knots but the mean error of kinetic energy is -5 knots. Nevertheless it seems likely that a modification of the computations which leads to improved forecasts of kinetic energy is likely to be accompanied by an improvement in the other statistics.

One of the most likely reasons for an increase in kinetic energy is the introduction and amplification of short-wave features, since the kinetic energy is proportional to the square of the wave number. Experiments were therefore carried out on a number of occasions in which the computational scheme included smoothing at three-hour intervals throughout the forecast period; the smoothing operator was designed to reduce the amplitude of the shortest waves while retaining that of the longer waves and full details are given by Wallington¹¹. Table V gives the mean statistics for 35 cases in which the smoothed forecasting procedure

TABLE V. *Mean statistics for smoothed and unsmoothed
1000 mb 30 hr forecasts for 0600 GMT verified against C.F.O. chart (35 cases)*

	Numerical forecast unsmoothed	Numerical forecast smoothed	C.F.O. forecast	Persistence
1.	0.55	0.53	0.71	—
2.	58	54	39	53
3.	24	19	16	21
4.	0.60	0.65	0.70	0.51
5.	20	12	—7	—2

1. Correlation coefficient between forecast and actual contour height changes
2. R.m.s. error in forecast contour heights (m)
3. R.m.s. vector error in forecast geostrophic wind (kt)
4. Stretch vector correlation between forecast and verifying geostrophic wind
5. Equivalent wind difference between forecast and verifying geostrophic wind (kt)—see p. 13.

was carried to give a 30-hour forecast at 1000 mb and for which corresponding statistics for the C.F.O. forecast were available. As judged by these statistics the smoothed forecasts were clearly superior to the unsmoothed as far as winds were concerned, the r.m.s. vector wind error having dropped from 24 knots to 19 knots, and the kinetic energy error from 20 knots to 12 knots while the stretch vector correlation coefficient had risen from 0.60 to 0.65. As expected, the kinetic energy error was considerably reduced, although in the mean positive, and is about twice the negative error made by C.F.O. The r.m.s. height error and the correlation between the forecast and actual height changes were almost unchanged when smoothing was introduced.

Table VI gives the mean statistics for 25 cases in which the smoothed and unsmoothed 24-hour forecasts for 0000 GMT were verified against the objective analysis for that time.

TABLE VI. *Mean statistics for smoothed and unsmoothed 24 hr forecasts for 0000 GMT verified against objective analyses (25 cases)*

	1000 mb	1000-500 mb	500 mb	500-200 mb	200 mb
1. Unsmoothed	0.71	0.79	0.76	0.61	0.78
Smoothed	0.71	0.84	0.79	0.67	0.83
2.	46	45	50	47	59
	43	34	45	38	49
3.	19	23	21	26	27
	16	15	17	15	17
4.	0.72	0.69	0.83	0.37	0.80
	0.76	0.76	0.87	0.50	0.87
5.	14	21	19	20	26
	6	-1	10	-4	11

1. Correlation coefficient between forecast and actual contour height changes
 2. R.m.s. error in forecast contour heights (m)
 3. R.m.s. vector error in forecast geostrophic wind (kt)
 4. Stretch vector correlation between forecast and verifying geostrophic wind
 5. Equivalent wind difference between forecast and verifying geostrophic wind (kt)—see p. 13
- In each case the statistic for the unsmoothed forecasts is given first.

At 1000 mb the statistics again show that smoothing improves the wind forecasts while leaving the other statistics almost unchanged. (The statistical measures given in Table VI are better than those given in Table V because the latter refer to a 30-hour forecast.) It is clear that smoothing is effective in improving the verification figures for the 1000-500 mb layer for the correlation between height changes and r.m.s. height error in addition to those concerning the wind forecasts. The most remarkable of these improvements are the notable decreases in the r.m.s. vector wind error and the kinetic energy error. At 500 mb the improvements in the wind statistics are not so noticeable as in the 1000-500 mb layer, but there is a marked reduction in the kinetic energy error. The kinetic energy errors above 500 mb are similarly affected by smoothing and the r.m.s. vector wind errors are considerably reduced. There can be no doubt that smoothing is an effective means of improving the wind forecasts, as measured by these statistics, and is generally beneficial as regards the r.m.s. height errors and the correlation between the forecast and actual height changes.

The numerical and conventional forecasts were compared with the verifying charts by synoptic meteorologists; there were no significant differences in the assessments by individuals so that there was no difficulty in collating them. Table VII gives the results of the assessments on 85 occasions. From this table we may infer that the numerical forecasts were satisfactory as routine forecasts on the occasions in categories 3, 4 and 5, i.e. on 46 occasions and that small improvements would lead to the inclusion of the remaining 17 occasions in category 2, i.e. on 63 occasions. It is clear that on many occasions there was little to choose between the forecasts but that on the remainder of occasions there was a preponderance of more useful conventional forecasts than vice versa.

TABLE VII. *Assessment by synoptic meteorologists (85 occasions)*

	no. of occasions
1. Numerical forecast worse than conventional forecast	22
2. Numerical forecast slightly worse than conventional forecast	26
3. Forecasts of equal merit	28
4. Numerical forecast better than conventional forecast	9
Total	85
5. Numerical forecast slightly worse than conventional forecast but both good forecasts (namely a selection of those in category 2)	9

SOME EXAMPLES OF THE NUMERICAL FORECASTS

Some examples of the numerical forecasts are given here mainly to illustrate the effects of various sources of errors. It has not been thought necessary to reproduce the charts at all levels for a particular occasion and attention is focused on the final prediction at the surface.

3 March 1961

Figures 5(a) and 5(b) show the surface charts at 0000 GMT on 3 March 1961, and at 0600 GMT on 4 March 1961, respectively and Figure 5(c) shows the numerical forecast for the latter time. The outstanding error in the numerical forecast is the development of the high-pressure cell to the west of Ireland and consequent north-westerly winds over the British Isles. Examination of the charts revealed that there was an error of transcription of the 0600 GMT upper winds at Ocean Weather Ship "D" owing to incorrect interpretation of the coded message whereby the wind at 5000 feet was used as that at 500 mb. The 0600 GMT analysis was thus based on a 500 mb wind of 32 knots from 180° instead of 86 knots from 260°. The 500 mb analysis used in the forecast is shown in Figure 5(d), the corrected analysis in Figure 5(e) and a surface forecast based on the corrected analysis in Figure 5(f). The two 500 mb analyses are remarkably different in the vicinity of O.W.S. "D" and additionally the southerly component of the thermal wind and the anticyclonic vorticity in the ridge were erroneously increased by the wrong observation. The forecast shown in Figure 5(f) is much more successful than that based on the incorrect analysis; in particular the westerly flow west of Ireland is properly indicated. It should be noted that the analysis with the

correct wind shows a region south of O.W.S. "D" where the contour gradient is slack; this is probably an error caused by the system adopted to make use of the few scattered upper wind observations available for 0600 GMT. The system allows an isolated wind to affect the gradient equally in both directions, although in this case the winds south of O.W.S. "D" were probably weaker than those to the north. The adjustment of contour gradients to accommodate isolated wind observations is an analysis problem which has not yet been solved satisfactorily.

30 March 1961

The surface charts at 0000 GMT, 30 March 1961, and 0600 GMT, 31 March 1961, are shown in Figures 6(a) and 6(b), and the numerical prediction for the latter time is shown in Figure 6(c). The particular error to which attention is drawn is the movement of the low-pressure system which was initially near north Scotland and which moved rapidly to 30°E with little deepening. The numerical forecast shows a movement to 15°E and a deepening to 985 mb. The assumed boundary conditions at the eastern edge of the forecasting area prevented the prediction of the correct pressure fall near the boundary and the low-pressure area was held back and its central pressure deepened; at the same time short-wave features were introduced into the computations. Figure 6(d) shows the smoothed numerical prediction, from which the short-wave features have been eliminated. The smoothed forecast is more successful in predicting the pressure level and replaces the low over Germany by a trough extending to the east.

10 January 1961

The initial and final surface charts are shown in Figures 7(a) and 7(b) and the numerical forecast for 0600 GMT, 11 January 1961 in Figure 7(c). The main features on the initial chart are the depression east of Canada, the mid-Atlantic ridge, the depression south of Ireland and the trough of low pressure over the European coastline. The depression south of Ireland moved south-east and at the same time a low-pressure area developed over Essex and drifted eastwards; the surface chart at 0600 GMT, 11 January 1961 shows a complex low-pressure system extending from east of Spain to Scandinavia. The mid-Atlantic ridge moved over the British Isles while the Canadian low moved to the south-east of Greenland. All these movements were successfully predicted by the numerical forecast, although the pressure levels were not so accurately predicted.

CONCLUSIONS

The experiment showed that it is possible to make numerical predictions on an operational basis, but that to do so would require a computer which is more reliable than METEOR, because short delays, for any reason, make it impossible to maintain the time schedule and produce the numerical forecast on time. The programmes and the data for the model used required all the storage space available in METEOR and any extension in complexity of the model or of the area covered by the forecast would make it necessary to use a computer which is both larger in capacity and faster in speed of operation than METEOR.

The statistical results and visual examination of the forecast charts both showed that the numerical forecasts were not as successful as those made by more conventional means, but that relatively small improvements in the analysis and in the model would be sufficient to reverse this position. Some of the necessary improvements are outside the dynamical model; for example, one of the most necessary is an increase in accuracy of data handling, which may

eventually be achieved by using the computer extensively for sorting and detecting errors in the data.

The consistent error of the numerical forecasts was the increase in kinetic energy; about half of this increase was due to the short-wave components and when these were controlled, by smoothing, there was an immediate improvement, although small-scale features of the synoptic situation may be lost in the process.

BIBLIOGRAPHY

1. KNIGHTING, E., CORBY, G. A., BUSHBY, F. H. and WALLINGTON, C. E.; An experiment in numerical forecasting. *Sci. Pap. met. Off., London*, No. 5, 1961.
2. KNIGHTING, E. and HINDS, M. K.; A report on some experiments in numerical prediction using a stream function. *Quart. J. R. met. Soc., London*, **86**, 1960, p. 504.
3. BUSHBY, F. H. and WHITELAM, C. J.; A three-parameter model of the atmosphere suitable for numerical integration. *Quart. J. R. met. Soc., London*, **87**, 1961, p. 374.
4. CORBY, G. A.; Some experiments in the objective analysis of contour charts. *Quart. J. R. met. Soc., London*, **87**, 1961, p. 34.
5. KNIGHTING, E.; Numerical forecasts made with two- and three-parameter models. *Met. Mag., London*, **90**, 1961, p. 117.
6. BUSHBY, F. H. and HINDS, M. K.; Further computations of 24-hr pressure changes based on a two-parameter model. *Quart. J. R. met. Soc., London*, **81**, 1955, p. 396.
7. BUSHBY, F. H. and HUCKLE, V. M.; Objective analysis in numerical forecasting. *Quart. J. R. met. Soc., London*, **83**, 1957, p. 232.
8. CRESSMAN, G. P.; An operational objective analysis system. *Mon. Weath. Rev., Washington, D.C.*, **87**, 1959, p. 367.
9. MURRAY, R.; On the accuracy of contour charts in forecasting upper winds. *Prof. Notes. met. Off., London*, 7, No. 110, 1954.
10. WALLINGTON, C. E.; An experiment in the verification of forecast charts. *Sci. Pap. met. Off., London*, No. 9, 1961.
11. WALLINGTON, C. E.; The use of smoothing or filtering operators in numerical forecasting. (Awaiting publication).

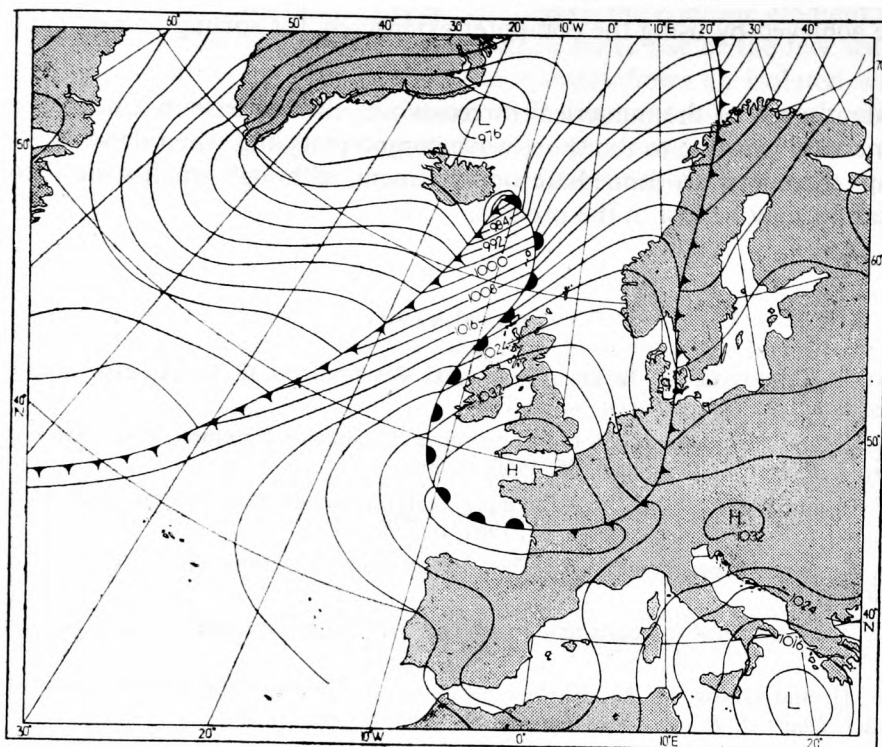


FIGURE 5(a). Actual surface chart for 0000 GMT, 3 March 1961—subjective (C.F.O.) analysis

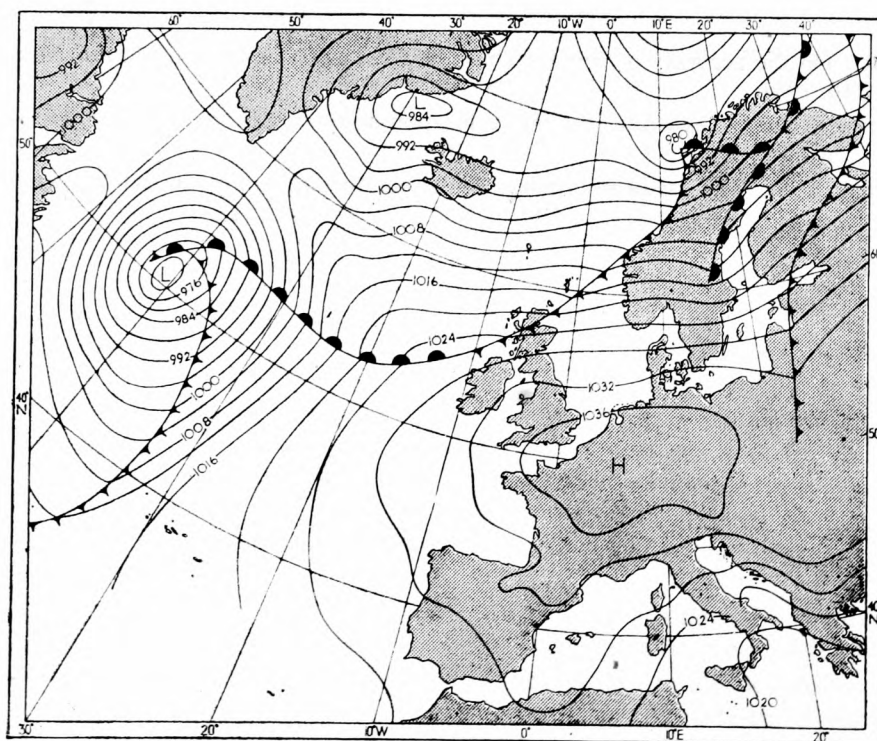


FIGURE 5(b). Actual surface chart for 0600 GMT, 4 March 1961—subjective (C.F.O.) analysis

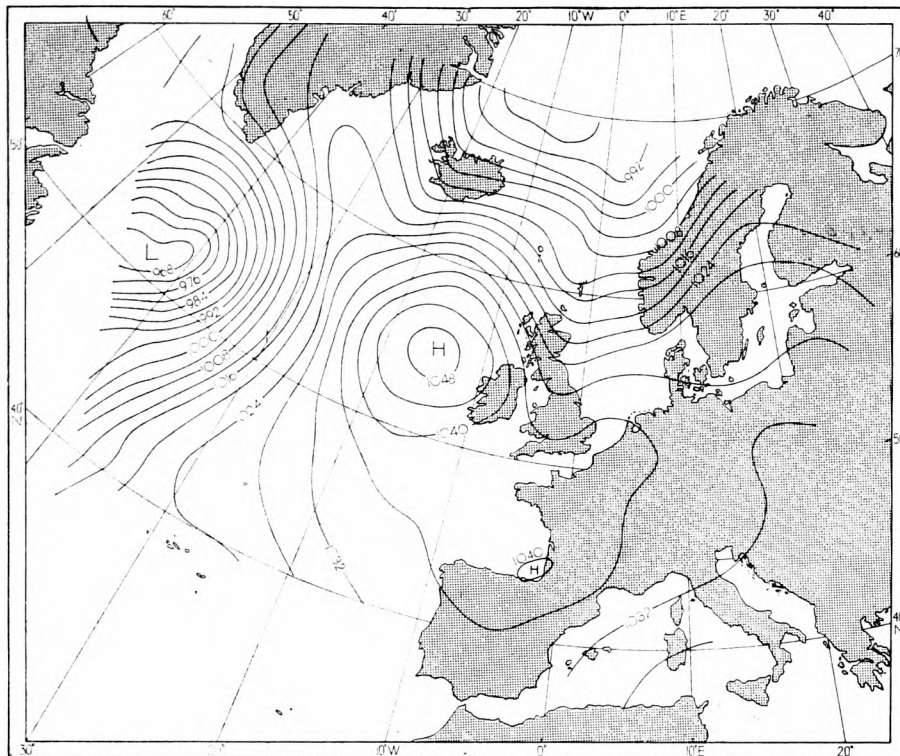


FIGURE 5(c). Numerical forecast of surface chart for 0600 GMT, 4 March 1961 based on objective analyses for 0000 and 0600 GMT, 3 March 1961

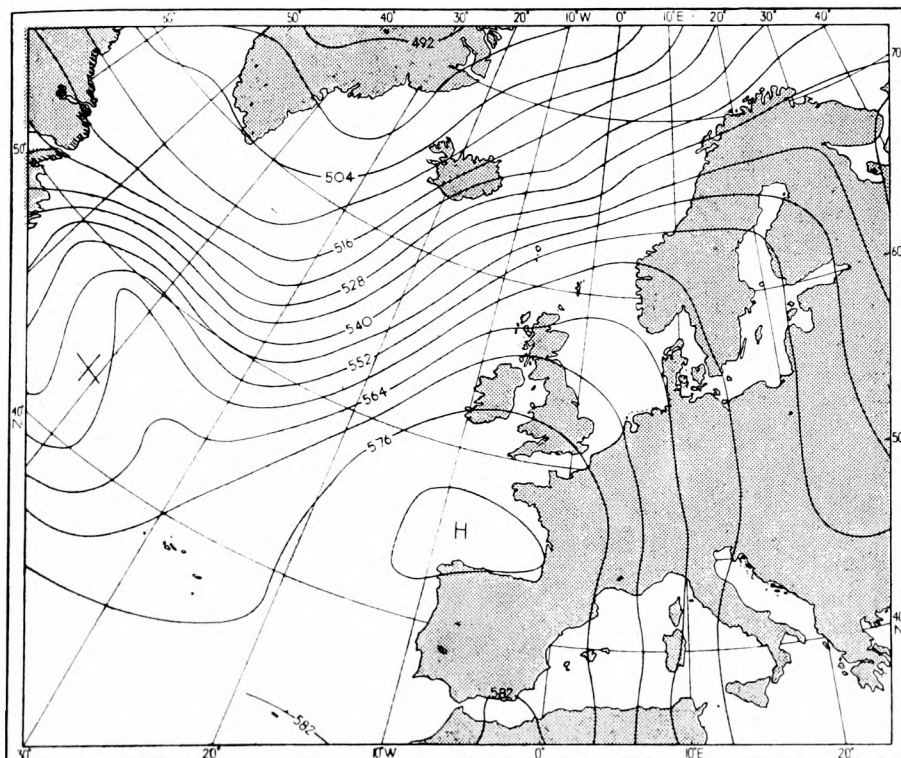


FIGURE 5(d). 500 mb objective analysis for 0600 GMT, 3 March 1961
An erroneous wind observation from O.W.S. "D" (marked with a cross) was used

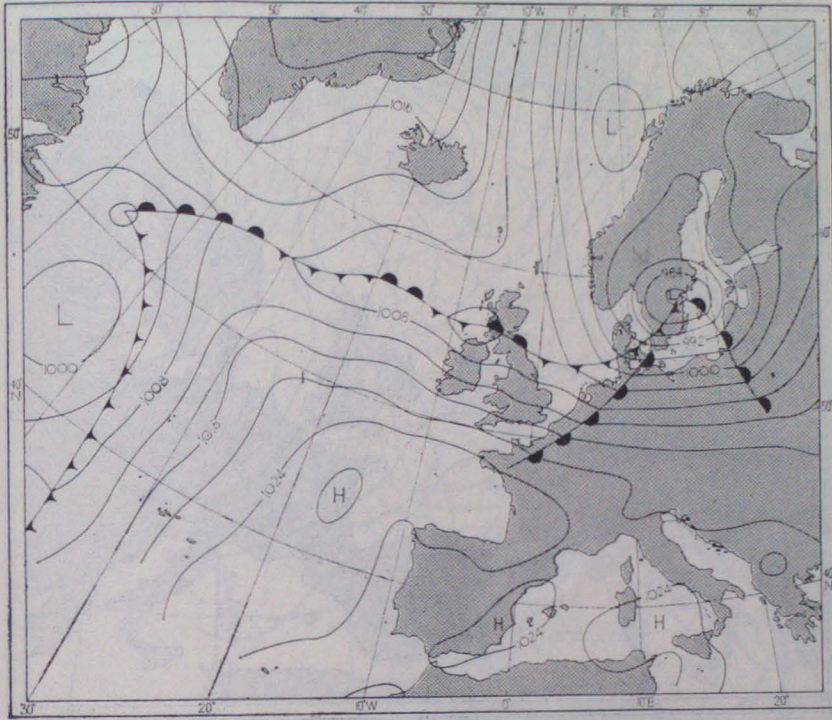


FIGURE 6(a). Actual surface chart for 0000 GMT, 30 March 1961—subjective (C.F.O.) analysis

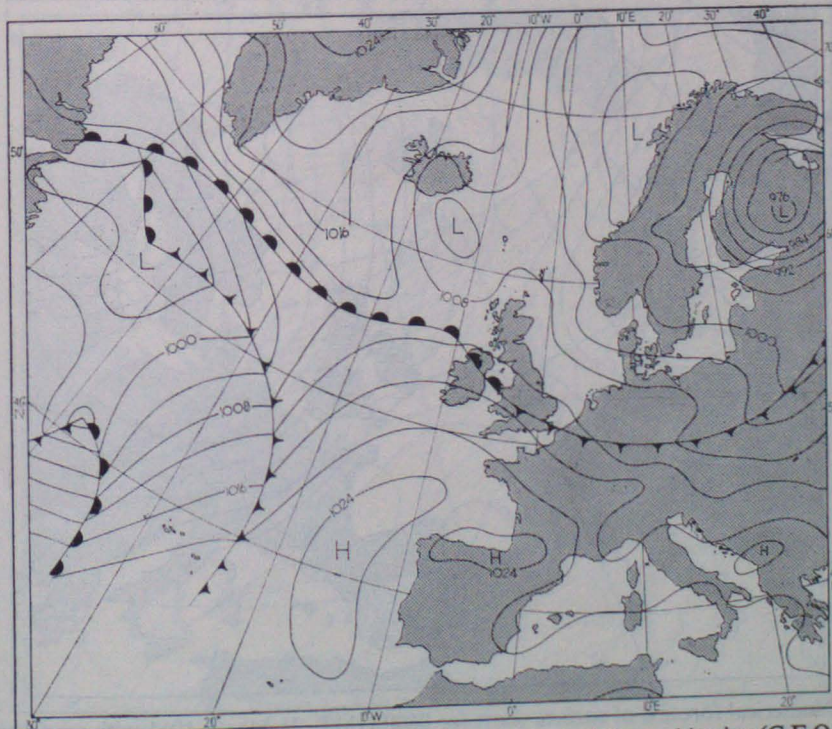


FIGURE 6(b). Actual surface chart for 0600 GMT 31 March 1961—subjective (C.F.O.) analysis

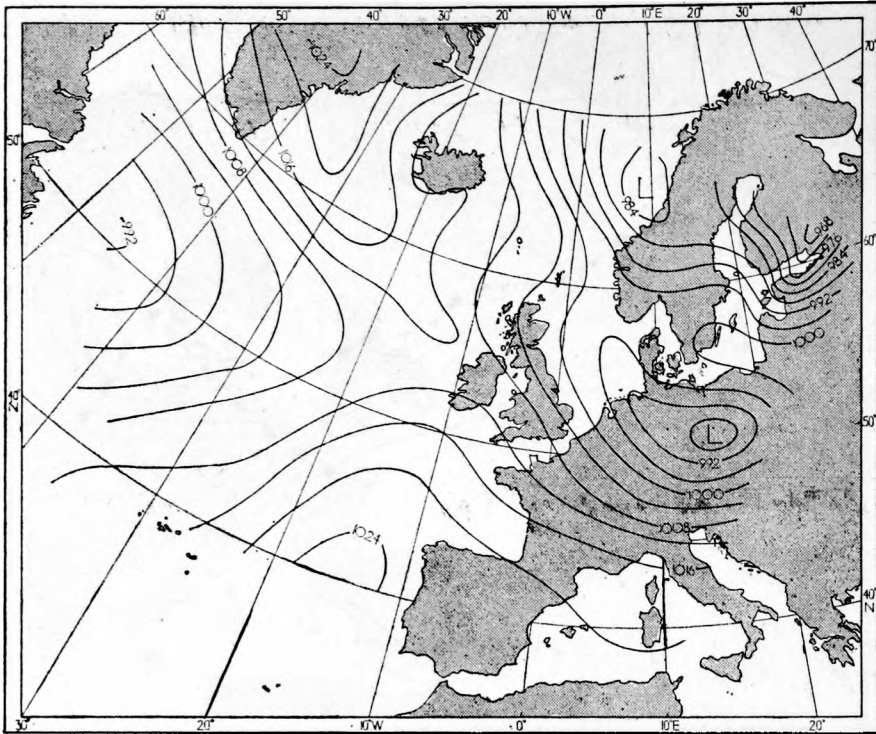


FIGURE 6(c). Numerical forecast of surface chart for 0600 GMT, 31 March 1961 using normal (unsmoothed) technique

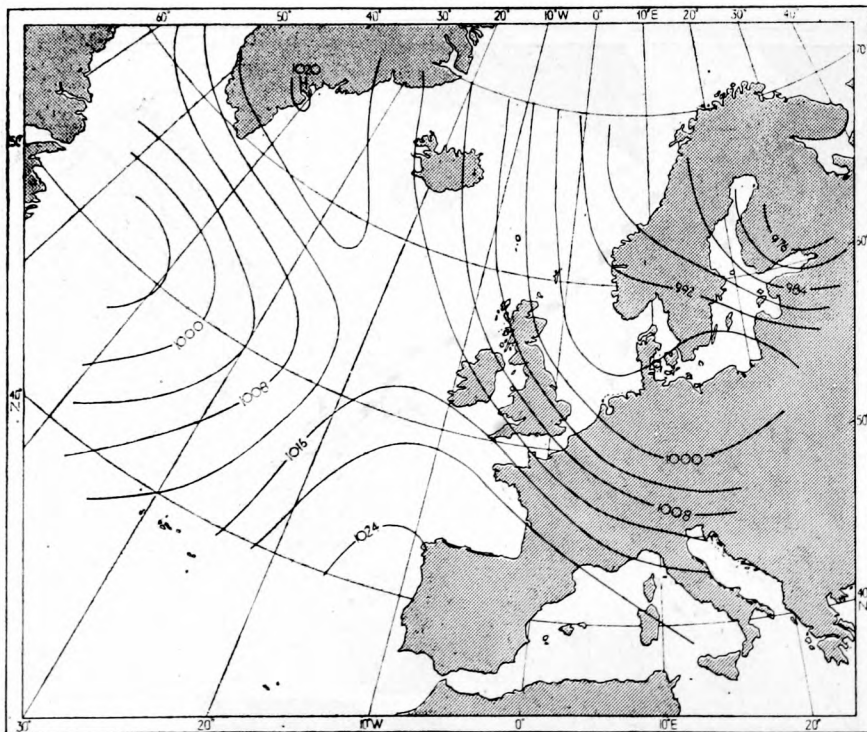


FIGURE 6(d). Numerical forecast of surface chart for 0600 GMT, 31 March 1961 with smoothing operator applied at intervals during the forecast

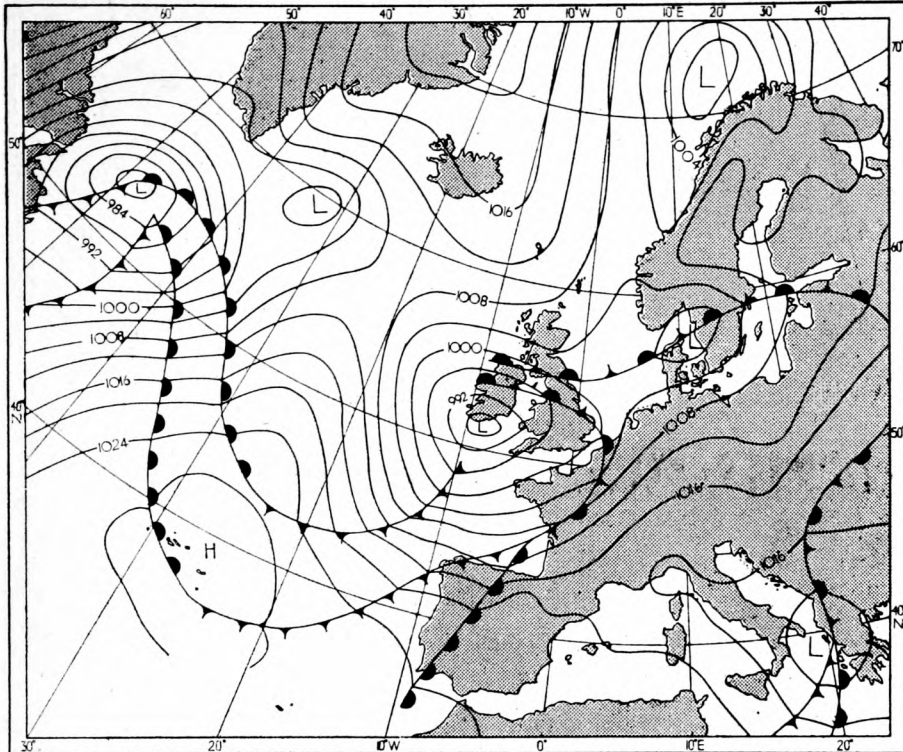


FIGURE 7(a). Actual surface chart for 0000 GMT, 10 January 1961—subjective (C.F.O.) analysis

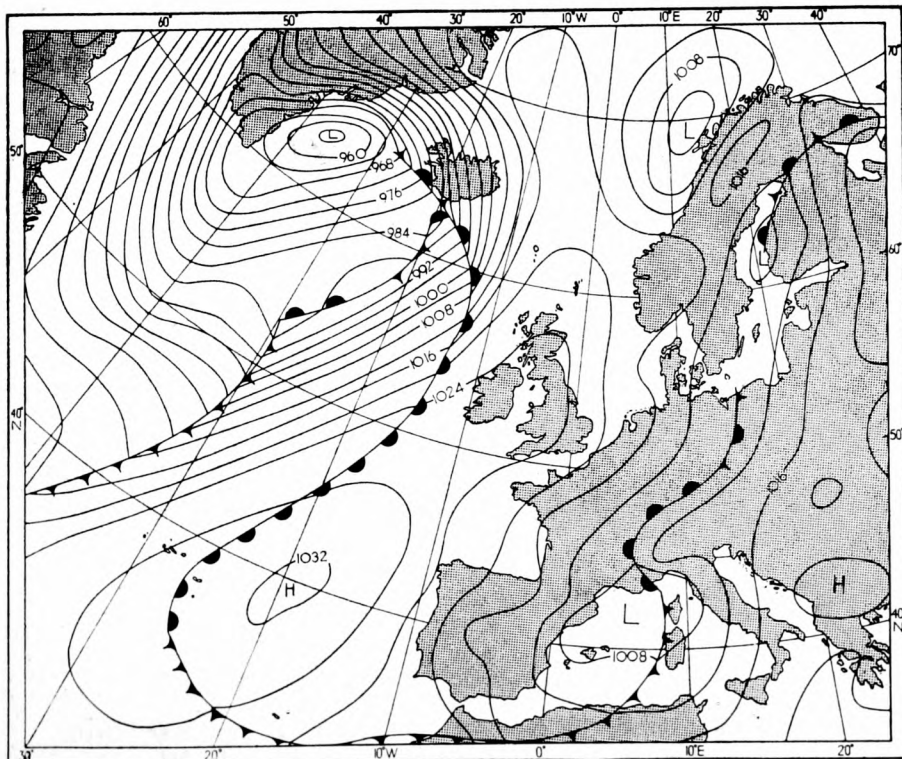


FIGURE 7(b). Actual surface chart for 0600 GMT, 11 January 1961—subjective (C.F.O.) analysis

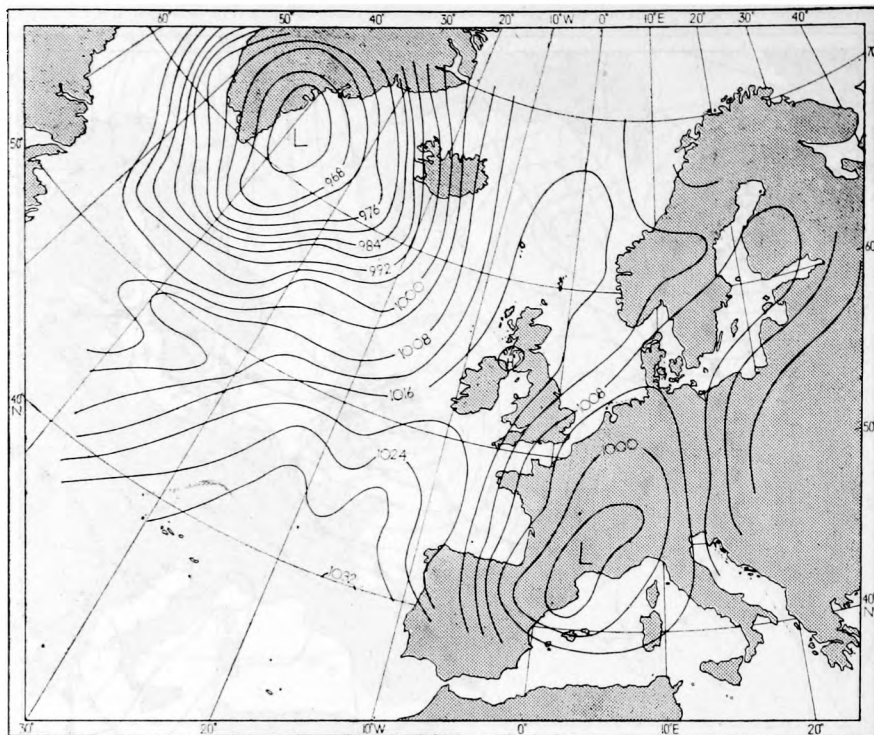


FIGURE 7(c). Numerical forecast of surface chart for 0600 GMT, 11 January 1961

Printed in England under the authority of HER MAJESTY'S STATIONERY OFFICE
by Dawson & Goodall Ltd., Grove Street, Bath, Somerset

© *Crown copyright* 1962

Published by
HER MAJESTY'S STATIONERY OFFICE

To be purchased from
York House, Kingsway, London, w.c.2
423 Oxford Street, London, w.1
13A Castle Street, Edinburgh 2
109 St. Mary Street, Cardiff
39 King Street, Manchester 2
50 Fairfax Street, Bristol 1
35 Smallbrook, Ringway, Birmingham 5
80 Chichester Street, Belfast 1
or through any bookseller